Enhancing Performance of Single-Channel SSVEP-Based Visual Acuity Assessment via Mode Decomposition

Xiaowei Zheng, Xun Zhang, Guanghua Xu, *Member, IEEE*, and Rui Zhang

Abstract— This study aimed to improve the performance of single-channel steady-state visual evoked potential (SSVEP)-based visual acuity assessment by mode decomposition methods. Using the SSVEP dataset induced by the vertical sinusoidal gratings at six spatial frequency steps from 11 subjects, 3-40-Hz band-pass filtering and other four mode decomposition methods, i.e., empirical mode decomposition (EMD), ensemble empirical mode decomposition (EEMD), improved complete ensemble empirical mode decomposition with adaptive noise (ICEEMDAN), and variational mode decomposition (VMD), were used to preprocess the single-channel SSVEP signals from Oz electrode. After comparing the SSVEP signal characteristics corresponding to each mode decomposition method, the visual acuity threshold estimation criterion was used to obtain the final visual acuity results. The agreement between subjective Freiburg Visual Acuity and Contrast Test (FrACT) and SSVEP visual acuity for band-pass filtering (−0.095 logMAR), EMD (−0.112 logMAR), EEMD (−0.098 logMAR), ICEEMDAN (−0.093 logMAR), and VMD (−0.090 logMAR) was all pretty good, with an acceptable difference between FrACT and SSVEP acuity for band-pass filtering (0.129 logMAR), EMD (0.083 logMAR), EEMD (0.120 logMAR), ICEEMDAN (0.103 logMAR), and VMD (0.108 logMAR), finding that the visual acuity obtained by these four mode decompositions had a lower limit of agreement and a lower or close difference compared to the traditional band-pass filtering method. This study proved that the mode decomposition methods can enhance the performance of single-channel SSVEP-based visual acuity assessment, and also recommended ICEEEMDAN as the mode decomposition method for single-channel electroencephalography (EEG) signal denoising in the SSVEP visual acuity assessment.

Index Terms— Visual acuity, steady-state visual evoked potential, empirical mode decomposition, signal denoising.

I. INTRODUCTION

VISUAL acuity, a measure of the spatial resolution of the visual system, is one of the most important visual functions. However, the traditional psychophysical testing methods, e.g., Snellen letters and Landolt C charts [1], are not suitable for preverbal children, the mentally disabled, and malingerers, since they require the examinees to have sufficient intelligence to abide by the test rules [2], [3].

Steady-state visual evoked potentials (SSVEPs) have been used as an objective diagnostic method regarding visual function [4]. In the SSVEP visual acuity technique, the widely used process of assessment contains several parts, i.e., visual stimuli, electroencephalography (EEG) acquisition, signal analysis, and acuity threshold determination. First, SSVEPs are induced by a series of visual stimuli with spatial frequency sweeping over time. Next, EEG signals are recorded and then processed by signal analysis algorithm, e.g., Fourier transform. Finally, the threshold determination criterion is applied to define the visual acuity threshold by establishing the relationship between the spatial frequency of the visual stimulus and SSVEP response [5]. As one of the most important parts of SSVEP visual acuity assessment, the threshold determination criterion is the visual acuity estimation method by SSVEP response against spatial frequency. Among them, the most widely used threshold determination criterion method is the linear extrapolation technique extrapolating the highest SSVEP response to 0 μV or noise level baseline between SSVEP response amplitude and spatial frequency [6].

Previous studies have proposed and compared the classic linear extrapolation methods and then improved these methods from some different aspects [7], e.g., machine learning [8], spatial filtering [9], and curvilinear form [10], [11]. Here, most studies use EEG signals from only a single channel in visual acuity assessment for its convenience, especially for children and infants, and then apply the Fourier transform to extract the frequency-domain amplitude feature [6]. However,

single-channel signals are more easily affected by the external environment and individual states, significantly affecting the visual acuity results [6]. Hence, it may potentially contribute to the performance of final SSVEP visual acuity results by eliminating noise and artifacts from single-channel EEG signals.

Empirical mode decomposition (EMD) is an adaptive signal processing method and has been extensively used in the analysis of non-stationary signals [12]. By using the EMD method, signals can be adaptively decomposed into a set of components, i.e., intrinsic mode functions (IMFs), which indicate the oscillation modes and reflect the characteristics of the signal itself. Recently, some improved methods of EMD have been put forward to solve the problem of mode mixing, e.g., ensemble empirical mode decomposition (EEMD) [13], complete ensemble empirical mode decomposition with adaptive noise (CEEMDAN) [14], improved CEEMDAN (ICEEMDAN) [15], and variational mode decomposition (VMD) [16]. In previous studies, EMD has been used in the EEG signal process field with pretty good performance [17], [18]. Since there is usually only one temporal frequency in SSVEP visual acuity assessment, EMD is theoretically suitable to eliminate artifact interference and some IMFs may concentrate around the stimulus frequency and its harmonics. By analyzing the IMF concentrating around the stimulus frequency, an SSVEP response with a higher signal-to-noise ratio (SNR) can be obtained, possibly improving the accuracy of visual acuity results. However, until now, little is known about the effect of denoising methods, e.g., mode decomposition, on the SSVEP visual acuity performance.

Therefore, this study aimed to explore the effect of mode decomposition methods on the single-channel SSVEP visual acuity assessment. First, the SSVEP dataset corresponding to six spatial frequencies and six electrode channels from 11 subjects was obtained from our previous study [9]. Then, EMD, EEMD, ICEEMDAN, and VMD were applied to the single-channel SSVEP signal of the Oz electrode, and the mode decomposition methods with good performance for further signal processing were chosen. Next, for each selected mode decomposition method, SSVEP visual acuity can be acquired by the threshold estimation criterion, and the statistical analyses were used to explore the performance of mode decomposition methods on SSVEP visual acuity.

II. MATERIALS AND METHOD

A. SSVEP Dataset

In this study, we used the SSVEP dataset in our previous work [9]. Eleven healthy subjects (four females, ages 22–27 years) were recruited. EEG was sampled by an EEG system (g.USBamp, g.tec, Schiedlberg, Austria) at six electrodes (O1, Oz, O2, PO3, POz, and PO4) with a 1200 Hz sampling frequency. As for the visual stimuli, the vertical sinusoidal gratings with a reversal frequency of 7.5 Hz were used with a Michelson contrast of 50% and a mean background luminance of 80 cd/m^2. The experimental process contained six blocks corresponding to six spatial frequencies of 3.0, 4.8, 7.5, 12.0, 19.0, and 30.0 cycles per degree (cpd) in

logarithmically equidistant steps for each eye. A total of fifteen eyes completed the test.

B. Mode Decomposition Methods

1) EMD: EMD is a data-driven and adaptive algorithm to analyze non-linear and non-stationary signals [12]. EMD decomposes a signal into a set of IMFs. As an effective IMF, it requires satisfying two conditions: (1) the numbers of extrema and zero-crossings are the same or differ at most by one; (2) the average of the upper envelope and lower envelope is zero at any point. Given any signal $x(t)$, the EMD algorithm can be described as follows:

(i) Find all local extrema of $x(t)$.

(ii) Interpolate all maxima/minima to obtain an upper/lower envelope $e_{max}(t)/e_{min}(t)$.

(iii) Compute the local mean by averaging envelops:

$$m_1(t) = (e_{max}(t) + e_{min}(t))/2. \tag{1}$$

(iv) Compute the IMF candidate by subtracting the local mean from the original data:

$$h_1(t) = x(t) - m_1(t). \tag{2}$$

(v) Check the properties of $h_1(t)$.

If $h_1(t)$ fulfills the conditions of IMF, $h_1(t)$ is regarded as an IMF, and it can be expressed as:

$$c_1(t) = h_1(t). \tag{3}$$

If $h_1(t)$ does not fulfill the conditions of IMF, $h_1(t)$ is treated as the original data:

$$x(t) = h_1(t). \tag{4}$$

Then repeat steps (i) to (v) above process until $h_1(t)$ becomes an IMF.

(vi) Compute the residue:

$$r_1(t) = x(t) - c_1(t). \tag{5}$$

Then treat r_1 as the new input data in step (i).

(vii) Repeat the procedure from (i) to (vii) for the subsequent residuals until the final residual satisfies the predefined stopping criterion, that is:

$$r_2(t) = r_1(t) - c_2(t)$$
$$\vdots$$
$$r_n(t) = r_{n-1}(t) - c_n(t). \tag{6}$$

Hence, the signal $x(t)$ can be decomposed into n IMFs and a residual:

$$x(t) = \sum_{i=1}^{n} c_i(t) + r_n(t). \tag{7}$$

2) EEMD: Mode mixing is the most significant drawback of EMD, which means either a single IMF consisting of signals of dramatically disparate scales or a signal of the same scale appearing in different IMF components. To overcome this problem, some improvements to EMD were proposed [19]. EEMD adds white noise into the IMFs decomposition process, and the bits of signals of different scales can be automatically designed onto proper scales of reference. This algorithm can be described briefly below:

(i) Add a white noise series to the original signal.

(ii) Decompose the signal containing added white noise into IMFs using EMD.

(iii) Repeat steps (i) and (ii) with various white noise series each time.

(vi) Obtain the ensemble means of corresponding IMFs of the decompositions as the final result, that is:

$$c_j(t) = \frac{1}{N} \sum_{k=1}^{N} \{c_{j,k}(t) + \alpha r_k(t)\}, \tag{8}$$

where $c_{j,k}(t) + \alpha r_k(t)$ is the kth decomposition of the jth IMF with the noise-added signal, N is the ensemble trials, α is the standard deviation of the white noise, and $r_k(t)$ is the residual after extracting k IMFs. In this study, α was set to 0.2, and N was set to 200.

3) ICEEMDAN: EEMD also has some drawbacks, e.g., each EMD decomposition does not necessarily generate the same number of IMFs, complicating the process of final averaging. Hence, CEEMDAN and ICEEMDAN were proposed. Here, this study concentrated on the ICEEMDAN method, which has overcome many of the problems associated with EEMD and was regarded as one of the most suitable methods for the analysis of EEG signals [20]. According to previous studies [15], [21], a brief introduction to ICEEMDAN is presented below:

(i) Let $E_k(\cdot)$ be the operator which produces the kth mode obtained by EMD. Let $\omega^{(i)}$ be the white noise and its ith average value and unit variance are zero. Let $M(\cdot)$ be the operation for calculating the mean value. For $x^i(t) = x(t) + \beta_0 E_1(w^i(t))$, calculate the mean value of results of I realizations via EMD, obtaining the first residual:

$$r_1(t) = M(x^i(t)), \tag{9}$$

where $\beta_0 = \varepsilon_0 \text{std}(x(t))/\text{std}(E_1(w^i(t)))$, and ε_0 is defined as the reciprocal of the desired signal to SNR between the first added noise and the analyzed signal.

(ii) Calculate the first mode at the first stage:

$$c_1(t) = x(t) - r_1(t). \tag{10}$$

(iii) Estimate the second residue as the mean of the realization $r_1(t) + \beta_1 E_2(w^i(t))$, and then the second mode can be defined:

$$c_2(t) = r_1(t) - r_2(t)$$
$$= r_1(t) - M(r_1(t) + \beta_1 E_2(w^i(t))). \tag{11}$$

(iv) Calculate the kth residue and kth mode ($k = 3, \ldots, K$):

$$r_k(t) = M(r_{k-1}(t) + \beta_{k-1} E_k(w^i(t))), \tag{12}$$

$$c_k(t) = r_{k-1}(t) - r_k(t). \tag{13}$$

(v) Go back to step (iv) for the next k until the resulting residual' no further decompositions can be performed.

4) VMD: VMD was proposed by Dragomiretskiy et al. [16], and it can non-recursively decompose a signal $f(t)$ into a discrete number of quasi-orthogonal sub-signals $u_k(t)$ compacting around a center frequency ω_k with limited bandwidth. The specific steps to resolve the bandwidth issue are as follows:

(i) Obtain the analytical signal and unilateral spectrum by applying the Hilbert transform to IMF:

$$\left(\sigma(t) + \frac{j}{\pi t}\right) \times u_k(t) \tag{14}$$

(ii) Multiplied by the exponential function $e^{-j\omega_k t}$, move the center band to the baseband:

$$\left[\left(\sigma(t) + \frac{j}{\pi t}\right) \times u_k(t)\right] \times e^{-j w_k t} \tag{15}$$

(iii) Estimate the bandwidth of the IMF by calculating the square of the L2 norm of the modulation signal gradient:

$$\min_{\{u_k\},\{\omega_k\}} \left\{ \sum_{k=1}^{K} \left\| \partial_t \left[\left(\delta(t) + \frac{j}{\pi t}\right) \times u_k(t)\right] e^{-j\omega_k t} \right\|_2^2 \right\}$$
$$\text{s. t.} \sum_{k=1}^{K} x_k(t) = x(t) \tag{16}$$

where $\{u_k\} = \{u_1, \ldots, u_K\}$ are the band-limited IMFs of the center frequency ω_k obtained by decomposition.

(iv) The above formula can be addressed by introducing a quadratic penalty and Lagrangian multipliers, The augmented Lagrangian is given as follows:

$$L(\{u_k\}, \{\omega_k\}, \lambda)$$
$$= \alpha \sum_{k=1}^{K} \left\| \partial_t \left[\left(\delta(t) + \frac{j}{\pi t}\right) \times u_k(t)\right] e^{-j\omega_k t} \right\|_2^2$$
$$+ \left\| f(t) - \sum_{k=1}^{K} u_k(t) \right\|_2^2 + \left\langle \lambda(t), f(t) - \sum_{k=1}^{K} u_k(t) \right\rangle \tag{17}$$

where α is the quadratic penalty factor, and λ is the Lagrange multiplier. Hence, this problem can be solved with the alternate direction method of multipliers (ADMM) [22]. The modes gained from solutions frequency-domain can be described below:

$$\hat{u}_k^{n+1}(w) = \frac{\hat{f}(w) - \sum_{i \neq k} \hat{u}_i(w) + \hat{\lambda}(w)/2}{1 + 2\alpha(w - w_k)^2} \tag{18}$$

where $\hat{u}_k^{n+1}(w)$, $\hat{f}(w)$, and $\hat{\lambda}(w)$ are obtained by the Fourier transform of $u_k^{n+1}(w)$, $f(w)$, and $\lambda(w)$; $\hat{u}_k^{n+1}(w)$ is the output after $\hat{f}(w) - \sum_{i \neq k} \hat{u}_i(w)$ wiener filtering. w_k is computed at the center of gravity of the corresponding mode's power spectrum, and w_k is updated using the formula below.

$$\omega_k = \frac{\int_0^{\infty} \omega |\hat{u}_k(\omega)|^2 d\omega}{\int_0^{\infty} |\hat{u}_k(\omega)|^2 d\omega} \tag{19}$$

C. Signal Processing

Firstly, we chose the Oz electrode as the analyzing single-channel signal [23], and the SSVEP data segments were extracted following the start and end times of each trial. Next, five different preprocessing methods, i.e., 3-40 Hz band-pass filter, EMD, EEMD, ICEEMDAN, and VMD, were used, and then the IMFs containing the stimulus frequency of 7.5 Hz were chosen for further processing. Next, the Fourier transform was carried out to extract the SSVEP features, and the amplitude at 7.5 Hz on the frequency-domain spectrum was regarded as the SSVEP amplitude. Besides, the signal noise was defined by the mean value of the 20 adjacent amplitudes of either side of the fundamental frequency of 7.5 Hz on the frequency-domain spectrum, and then SNR can be described as:

$$SNR = \frac{\text{NSVEP amplitude}}{\text{Noise}}$$
$$= \frac{a(f)}{\frac{1}{10} * \sum_{k=1}^{k=10} a(fk * \Delta f)a(f - k * \Delta f)} \quad (20)$$

in which $a(f)$ denotes the frequency-domain amplitude at frequency f, and the frequency resolution Δf is 0.1 Hz.

For the SSVEP-based visual acuity definition, the estimation criterion of linear extrapolation to noise level baseline was also used in this study [7], [23]. After plotting SSVEP amplitude versus spatial frequency, a regression line can be extrapolated from the last significant SSVEP peak to a noise level baseline. The SSVEP visual acuity was defined as the spatial frequency corresponding to the intersection point of the regression line and the noise level baseline. The significance of the SSVEP response was judged by the preset SNR level, and the noise level baseline was defined as the mean of the noise of the six spatial frequency steps.

D. Statistical Analyses

The agreement and difference between the psychophysical FrACT and objective SSVEP visual acuity were evaluated by Bland–Altman analysis for each mode decomposition method. Besides, the SNR difference among each preprocessing mode decomposition method was evaluated by one-way repeated-measures ANOVA, and the *post-hoc* analysis with Bonferroni correction for multiple comparisons was subsequently employed.

III. RESULT

A. Mode Decomposition Methods

Five methods, i.e., the band-pass filter of 3-40 Hz, EMD, EEMD, ICEEMDAN, and VMD, were used to preprocess single-channel EEG signals from the Oz electrode, respectively. As shown in Fig. 1, all four mode decomposition methods can decompose the original signal into several IMFs, and at least one IMF has a significant peak at the stimulus frequency of 7.5 Hz in the frequency-domain, demonstrating mode decomposition methods can be used as a signal denoising method for SSVEPs. For example, as shown in Fig. 1(a), the EMD method decomposes the original signal into six IMFs and one residual signal, and IMF2 and IMF3 show a significant
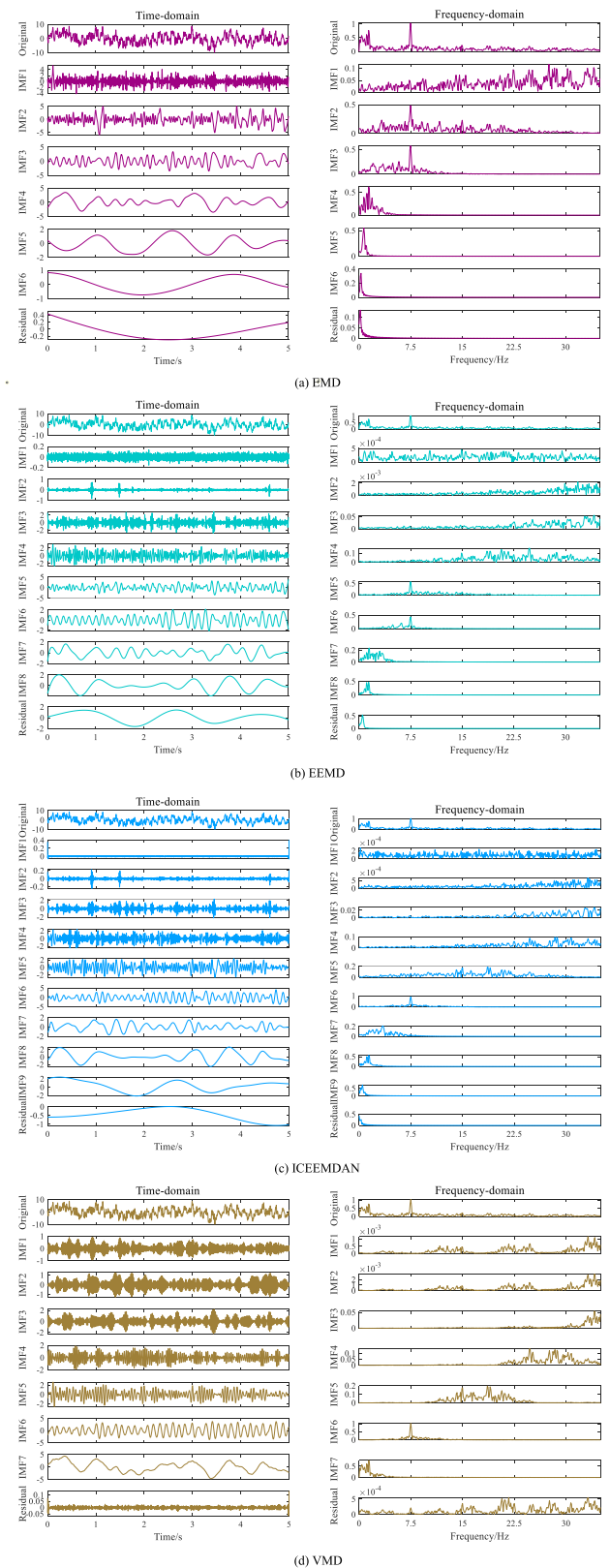

Fig. 1. IMF decomposition diagram and frequency spectrum from Oz single-channel signal at 3.0 cpd (subject S9, right eye). (a) EMD. (b) EEMD. (c) ICEEMDAN. (d) VMD.

response peak at the stimulus frequency of 7.5 Hz in the frequency-domain, Hence, the IMF2 and IMF3 were used to regenerate new signal to reduce noise. Likewise, the IMF5 and
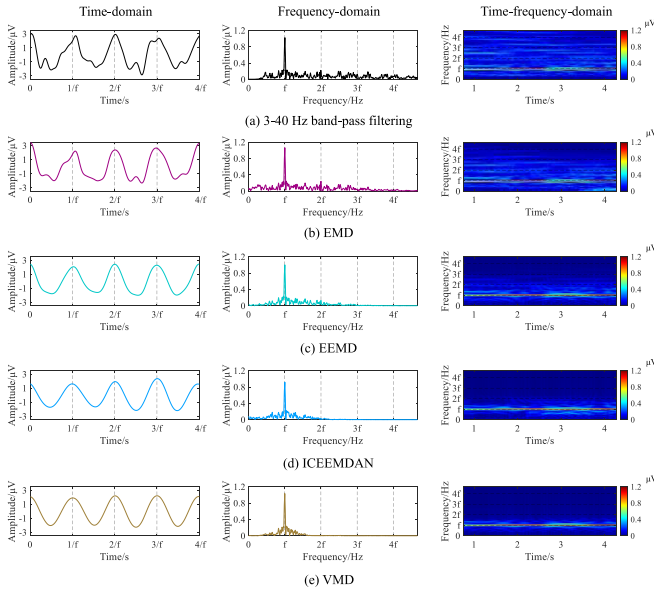
Fig. 2. Time-domain, frequency-domain, and time–frequency-domain analyses of regenerated SSVEPs at 3.0 cpd. (a) 3-40 Hz band-pass filtering. (b) EMD. (c) EEMD. (d) ICEEMDAN. (e) VMD. "f" in all subfigures represents the stimulus frequency of 7.5 Hz.

IMF6 of EEMD, the IMF6 of ICEEMDAN, and the IMF7 of VMD were used to regenerate new signals, respectively.

B. SSVEP Response Performance

Fig. 2 shows the time-domain, frequency-domain, and time-frequency-domain analyses of the regenerated SSVEPs in Fig. 1. For time-domain analyses, the 5-s single-channel regenerated signals were averaged to obtain the 0.53-s non-overlapping data segments with each segment containing four periods of a 7.5 Hz reversal process. For frequency-domain analyses, the Fourier transform was carried out for 5-s regenerated signals. For the time-frequency-domain analyses, the 2.0-s window length with 0.1-s sliding length over the 5-s regenerated signals was used to obtain the time-frequency-domain characteristics.

The time-domain waveforms and frequency-domain spectrums show all the regenerated signals after being preprocessed by the five methods, i.e., 3-40 Hz band-pass filtering, EMD, EEMD, ICEEMDAN, and VMD, had the main periodicity at the fundamental reversal frequency of 7.5 Hz. Compared to 3-40 Hz band-pass filtering and EMD, the signals preprocessed by EEMD, ICEEMDAN, and VMD had a higher energy concentration at 7.5 Hz, as shown in time-frequency-domain analyses, indicating that the mode decomposition methods suppressed the artifact noise of the original EEG signal, and thereby enhancing the SNR.

C. Mode Decomposition Effect

The mode decomposition effect aims to suppress the non-SSVEP components to enhance SNR. Hence, here, this study mainly compared the SNR values of various mode decomposition methods to judge the mode decomposition effect. As shown in Fig. 3, the amplitude and SNR values corresponding to the spatial frequency of 3.0 cpd were compared
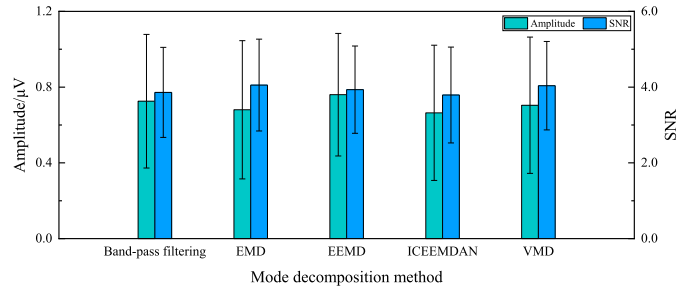

Fig. 3. Comparison of amplitude and SNR of regenerated SSVEPs at 3.0 cpd over all subjects.

since the visual stimuli at this spatial frequency were the clearest to all subjects. Fig. 3 shows that the SNR values from EMD (4.054±1.212), EEMD (3.933±1.153), and VMD (4.037±1.168), were higher than that of the traditional band-pass filtering (3.861±1.188), with ICEEMDAN had a slightly lower SNR (3.793±1.265). Then, one-way repeated-measures ANOVA found that there was a significant difference ($F_{(4,60)} = 4.611$, $P = 0.003$) in the SNR values of regenerated SSVEPs, and subsequently, the Bonferroni *post-hoc* analysis showed no difference between any pair of SNR values, demonstrating that the SNR values had a good agreement among these regenerated SSVEPs.

D. SSVEP Visual Acuity Estimation

SSVEP visual acuity threshold was defined by the corresponding spatial frequency of the intersection point between the noise level baseline and the regression line extrapolating from the significant SSVEP peak to the last data point with an SNR higher than the preset SNR level. For the band-pass filtering, the suggested value of the SNR level, i.e., 1.0, has been given by the previous studies [7], [24]. And then, as shown in Fig. 4, since the SNR values of SSVEPs regenerated from the mode decomposition methods had no difference from that of the band-pass filtering, the SNR level of 1.0 was also suitable for the four mode decomposition methods.

As shown in Fig. 5, the tuning curves of SSVEP visual acuity estimation criterion for 3-40 Hz band-pass filtering, EMD, EEMD, ICEEMDAN, and VMD can be obtained, respectively. The range for the linear regression is defined from the first data peak point. e.g., 1.140 μV in Fig. 5(a), to the last significant data point with an SNR higher than 1.0, e.g., 0.118 μV with an SNR of 1.508 in Fig. 5(a). Then the SSVEP visual acuity can be obtained as the spatial frequency of the intersection point of the regression line and the noise level baseline, e.g., 26.554 cpd in Fig. 5(a). Similar to this, the visual acuity thresholds for Fig. 5(b)-(e) were 26.431, 26.347, 25.312, and 26.217 cpd.

E. Visual Acuity Results

According to the process above, the SSVEP visual acuity over all subjects was obtained, as shown in Table I. Here, the unit of logMAR was used to express the final visual acuity results for its uniformity in spatial frequency [5], [23]. Since all the subjects had normal or corrected-to-normal

TABLE I
VISUAL ACUITY RESULTS OF FRACT AND SSVEP

Subject	Eye	Visual Acuity/logMAR					
		FrACT	Band-pass	EMD	EEMD	ICEEMDAN	VMD
S1	Right	-0.06	0.19	0.03	0.21	0.20	0.21
S2	Left	0.02	-0.13	0.12	0.04	0.04	0.04
S2	Right	-0.06	0.05	0.06	0.06	0.07	0.06
S3	Right	-0.04	0.06	0.06	0.12	0.21	0.06
S4	Left	-0.08	0.08	0.03	0.06	0.03	0.09
S4	Right	0.04	0.07	0.21	0.20	0.17	0.08
S5	Right	0.01	0.16	0.05	0.06	0.06	0.09
S6	right	-0.10	-0.18	0.06	0.07	0.07	0.10
S7	Left	0.11	0.18	0.11	-0.10	0.00	-0.08
S7	Right	-0.07	0.23	0.18	0.20	0.00	0.10
S8	Right	0.01	0.11	0.11	0.05	-0.06	0.02
S9	Left	-0.09	0.03	0.16	-0.05	0.00	0.01
S9	Right	0.00	-0.09	0.07	0.02	0.05	0.04
S10	Left	-0.09	0.19	0.07	0.09	0.09	0.09
S11	Right	0.05	0.10	0.00	0.10	0.10	0.10
Mean		-0.02	0.10	0.08	0.02	0.09	0.11
SD		0.06	0.12	0.06	0.08	0.07	0.06

TABLE II
RESULTS OF BLAND-ALTMAN ANALYSIS BETWEEN SUBJECTIVE
FRACT AND OBJECTIVE SSVEP VISUAL ACUITY. LoA-, THE
LOWER BOUND OF 95% LIMIT OF AGREEMENT; LoA+, THE
UPPER BOUND OF 95% LIMIT OF AGREEMENT

	Difference	SD	LoA-	LoA+
Band-pass	-0.095	0.129	-0.348	0.159
EMD	-0.112	0.083	-0.274	0.050
EEMD	-0.098	0.120	-0.333	0.137
ICEEMD	-0.093	0.103	-0.294	0.109
VMD	-0.090	0.108	-0.301	0.121

visual acuity, the visual acuity results were in the vicinity of 0.0 logMAR with a mean value of -0.02 ± 0.06 logMAR for the subjective FrACT test.

The reliability analysis of Bland-Altman was used to describe the difference and agreement between subjective FrACT and objective SSVEP visual acuity, as shown in Table II. The difference between FrACT and SSVEP visual acuity for band-pass filtering, EMD, EEMD, ICEEMDAN, and VMD were -0.095 ± 0.129 logMAR, -0.112 ± 0.083 logMAR, -0.098 ± 0.120 logMAR, -0.093 ± 0.103 logMAR, and -0.090 ± 0.108 logMAR with a 95% limit of agreement were 0.253, 0.163, 0.235, 0.202, and 0.212 logMAR, respectively.

Compared to FrACT visual acuity, these five SSVEP visual acuity all had a good agreement with it, demonstrating that mode decomposition methods had a good performance in the SSVEP visual acuity assessment. Besides, the visual acuity obtained by these four mode decompositions had a lower limit of agreement and a lower or close difference compared to the traditional band-pass filtering method, proving that the mode decomposition methods can enhance the performance of single-channel SSVEP-based visual acuity assessment. According to Table II, this study recommended ICEEEMDAN as the best choice of mode decomposition methods for single-channel EEG signal denoising in the SSVEP visual acuity assessment as it performed the lowest difference and lower limit of agreement.

IV. DISCUSSION

The main advantage of EMD is that it is a data-driven method to analyze non-stationary signals stemming from non-linear systems and no need to postulate the mother wavelet and level of decomposition as in wavelet transform [12]. Next, to overcome the limitation of mode-mixing, EEMD was first proposed, which performs the decomposition over an ensemble of noisy copies of the original signal, obtaining the final results by averaging [19]. Then, as an improvement on EEMD, CEEMDAN, and ICEEMDAN achieve a negligible reconstruction error and solve the problem of the different number of modes for different realizations of signal plus noise [14]. Compared to EMD and its variants EEMD and CEEMDAN, VMD can adaptively calculate the appropriate bands and gives a concurrent estimate of corresponding modes and a more robust and well-defined time-domain analysis [25].

There were some parameter settings required for EEMD, ICEEMDAN, and VMD in this study. For the settings of these parameters, there were two bases in this study. On one hand, a series of pre-experiments and pre-process were performed before the final parameters were determined. On the other hand, the relevant settings also referred to the previous studies. For EEMD and ICEEMDAN, the ensemble number was set to 200. For VMD, the main parameters contain penalty factor α, decomposition layer number K, fidelity coefficient τ, and termination condition ε. Decomposition layer number K is the most important parameter that influences VMD performance. Penalty factor α mainly influences the bandwidth of the frequency band. The fidelity coefficient τ can ensure the integrity of the signal after reconstruction. Here, according to previous studies [26], penalty factor α was to 2000; decomposition layer number K was set to 7; fidelity coefficient τ was set to 0.3; termination condition ε was to 10^{-7}.

This study mainly focused on the signal performance around the stimulus frequency of 7.5 Hz. As shown in Fig. 3, the mean SSVEP amplitude in mode decomposition methods showed a lower level except for EEMD, which may be caused by the mode-mixing meaning that other IMFs may also contain a little
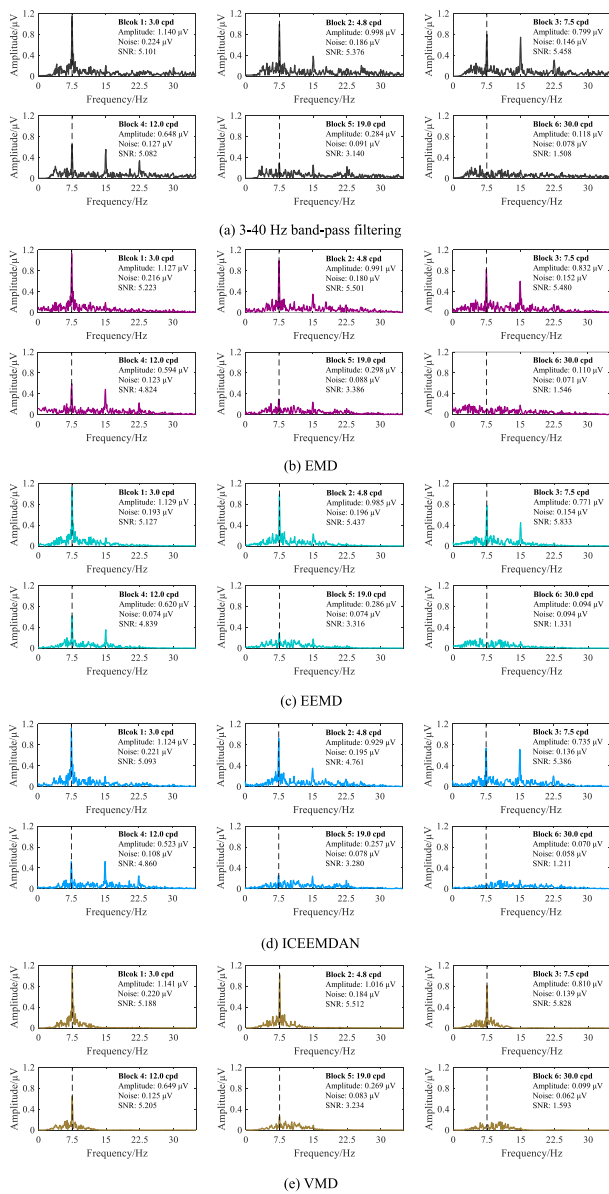
Fig. 4. Regenerated SSVEP response to six spatial frequency steps. (a) 3-40 Hz band-pass filtering. (b) EMD. (c) EEMD. (d) ICEEMDAN. (e) VMD.

Fig. 5. Tuning curves for SSVEP visual acuity estimation criterion. (a) 3-40 Hz band-pass filtering. (b) EMD. (c) EEMD. (d) ICEEMDAN. (e) VMD.

signal energy around 7.5 Hz. As for EEMD, the additional added white noise may cause a slightly higher amplitude. As for SNR, the EMD, EEMD, and VMD had slightly higher mean SNR than band-pass filtering, demonstrating that these mode decomposition methods suppress noise to a certain extent and enhance SNR.

As shown in Fig. 1, EMD and EEMD methods show a more severe mode mixing than ICEEMDAN and VMD. Even at the target frequency of 7.5 Hz, EMD and EEMD had obvious peaks in at least two different IMFs, showing that the simple EMD or EEMD method is insufficient in the decomposition of SSVEPs. As for ICEEMDAN and VMD, the single IMF contained the vast majority of SSVEP information, suggesting VMD or ICEEMDAN as a prior choice in decoding SSVEP patterns from EEG [26].

This study provides evidence of enhancing SSVEP visual acuity performance by mode decomposition, demonstrating
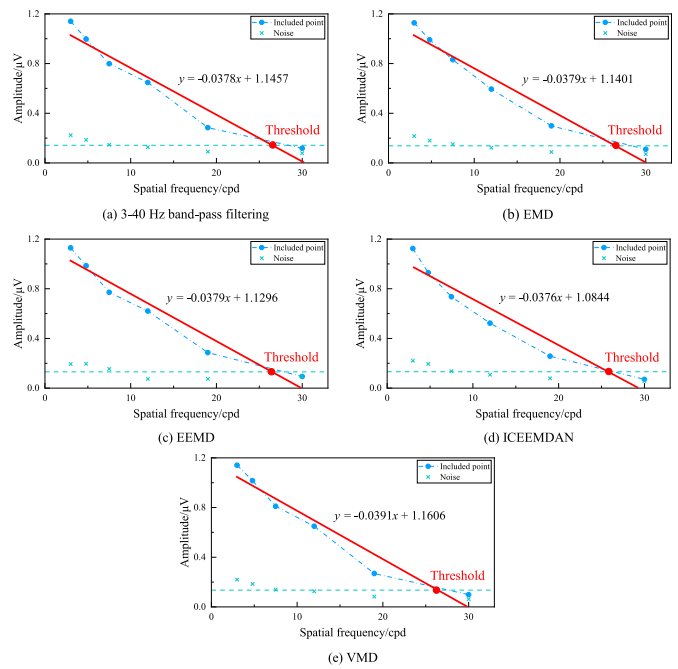
that the denoising methods may offer an alternative method to improve the SSVEP visual acuity assessment, and also showing that signal processing technology in the engineering field and clinical diagnosis technology in the medical field can be integrated to better serve human society. Besides, our previous study introduced spatial filtering in multi-channel visual acuity assessment, finding canonical correlation analysis-based SSVEP visual acuity had a better performance than the traditional single-channel method [9], and it also proves this hypothesis. Hence, in the future, other signal processing methods, i.e., empirical wavelet transform (EWT) [27], image filtering [28], and singular spectrum analysis (SSA) [29], can be used to further enhance the performance of SSVEP visual acuity assessment.

Some limitations must be addressed. First, although single-channel signals are more convenient to record, their validity is relatively easy to be affected by the system environment. Therefore, follow-up research on the validity of the data is necessary. Second, the best parameters setting of EEMD, ICEEMDAN, and VMD is related to the characteristics of the data itself and it may be affected by the SSVEP acquisition factors, e.g., the visual stimuli, the hardware equipment, and the subject. Hence, the previously recommended parameter settings may not be very suitable here, and future studies can focus on the parameter optimization process of mode decomposition methods. Third, some other factors, e.g., the data length of one trial, the trial number, the stimulus paradigm type, and the spatial frequency settings, may also influence the SSVEP visual acuity assessment results. Although the International Society for Clinical Electrophysiology of Vision (ISCEV) has recommended some set standards [23], [30], the standardization of clinical electrophysiology of vision also requires more joint effort by researchers.

V. CONCLUSION

This study introduced the mode decomposition methods, i.e., EMD, EEMD, ICEEMDAN, and VMD, in the single-channel SSVEP visual acuity assessment, finding that the visual acuity obtained by these four mode decompositions had a lower limit of agreement and a lower or close difference compared to the traditional band-pass filtering method. This study proved that the mode decomposition methods can enhance the performance of single-channel SSVEP-based visual acuity assessment, and also recommended ICEEEM-DAN as the mode decomposition method for single-channel EEG signal denoising in the SSVEP visual acuity assessment.

REFERENCES

[1] F. Ricci, C. Cedrone, and L. Cerulli, "Standardized measurement of visual acuity," *Ophthalmic Epidemiol.*, vol. 5, no. 1, pp. 41–53, Jan. 1998.

[2] R. R. A. Bourne et al., "Magnitude, temporal trends, and projections of the global prevalence of blindness and distance and near vision impairment: A systematic review and meta-analysis," *Lancet Global Health*, vol. 5, no. 9, pp. e888–e897, Sep. 2017.

[3] T. R. Fricke et al., "Global prevalence of presbyopia and vision impairment from uncorrected presbyopia: Systematic review, meta-analysis, and modelling," *Ophthalmology*, vol. 125, no. 10, pp. 1492–1499, Oct. 2018.

[4] A. M. Norcia, L. G. Appelbaum, J. M. Ales, B. R. Cottereau, and B. Rossion, "The steady-state visual evoked potential in vision research: A review," *J. Vis.*, vol. 15, no. 6, p. 4, May 2015.

[5] X. Zheng et al., "Assessment of human visual acuity using visual evoked potential: A review," *Sensors*, vol. 20, no. 19, p. 5542, Sep. 2020.

[6] R. Hamilton et al., "VEP estimation of visual acuity: A systematic review," *Documenta Ophthalmologica*, vol. 142, no. 1, pp. 25–74, Feb. 2021.

[7] X. Zheng et al., "Threshold determination criterion in steady-state visual evoked potential-based acuity assessment: A comparison of four common methods," *IEEE Access*, vol. 8, pp. 188844–188852, 2020.

[8] M. Bach and S. P. Heinrich, "Acuity VEP: Improved with machine learning," *Documenta Ophthalmologica*, vol. 139, no. 2, pp. 113–122, Oct. 2019.

[9] X. Zheng et al., "Enhancing performance of SSVEP-based visual acuity via spatial filtering," *Frontiers Neurosci.*, vol. 15, Aug. 2021, Art. no. 716051.

[10] T. Strasser et al., "Objective assessment of visual acuity: A refined model for analyzing the sweep VEP," *Documenta Ophthalmologica*, vol. 138, no. 2, pp. 97–116, Apr. 2019.

[11] A. Kurtenbach, H. Langrová, A. Messias, E. Zrenner, and H. Jägle, "A comparison of the performance of three visual evoked potential-based methods to estimate visual acuity," *Documenta Ophthalmologica*, vol. 126, no. 1, pp. 45–56, Feb. 2013.

[12] N. E. Huang et al., "The empirical mode decomposition and the Hilbert spectrum for nonlinear and non-stationary time series analysis," *Proc. Roy. Soc. London A, Math., Phys. Eng. Sci.*, vol. 454, no. 1971, pp. 903–995, Mar. 1998.

[13] Z. Wu, N. E. Huang, and X. Chen, "The multi-dimensional ensemble empirical mode decomposition method," *Adv. Adapt. Data Anal.*, vol. 1, no. 3, pp. 339–372, Jul. 2009.

[14] M. E. Torres, M. A. Colominas, G. Schlotthauer, and P. Flandrin, "A complete ensemble empirical mode decomposition with adaptive noise," in *Proc. IEEE Int. Conf. Acoust., Speech Signal Process. (ICASSP)*, May 2011, pp. 4144–4147.

[15] M. A. Colominas, G. Schlotthauer, and M. E. Torres, "Improved complete ensemble EMD: A suitable tool for biomedical signal processing," *Biomed. Signal Process. Control*, vol. 14, pp. 19–29, Nov. 2014.

[16] K. Dragomiretskiy and D. Zosso, "Variational mode decomposition," *IEEE Trans. Signal Process.*, vol. 62, no. 3, pp. 531–544, Feb. 2014.

[17] Y.-F. Chen, K. Atal, S.-Q. Xie, and Q. Liu, "A new multivariate empirical mode decomposition method for improving the performance of SSVEP-based brain–computer interface," *J. Neural Eng.*, vol. 14, no. 4, Aug. 2017, Art. no. 046028.

[18] A. Pradhan, "A survey of classification of EEG signals using EMD and VMD for epileptic seizure detection," *Int. J. Eng. Res.*, vol. 9, no. 5, pp. 495–498, May 2020.

[19] Z. Wu and N. E. Huang, "Ensemble empirical mode decomposition: A noise-assisted data analysis method," *Adv. Adapt. Data Anal.*, vol. 1, no. 1, pp. 1–41, Jan. 2009.

[20] R. A. Thuraisingham, "Revisiting ICEEMDAN and EEG rhythms," *Biomed. Signal Process. Control*, vol. 68, Jul. 2021, Art. no. 102701.

[21] X. Li and C. Li, "Improved CEEMDAN and PSO-SVR modeling for near-infrared noninvasive glucose detection," *Comput. Math. Methods Med.*, vol. 2016, Aug. 2016, Art. no. 8301962.

[22] M. R. Hestenes, "Multiplier and gradient methods," *J. Optim. Theory Appl.*, vol. 4, no. 5, pp. 303–320, Nov. 1969.

[23] R. Hamilton et al., "ISCEV extended protocol for VEP methods of estimation of visual acuity," *Documenta Ophthalmologica*, vol. 142, no. 1, pp. 17–24, Feb. 2021.

[24] N. K. Yadav, F. Almoqbel, L. Head, E. L. Irving, and S. J. Leat, "Threshold determination in sweep VEP and the effects of criterion," *Documenta Ophthalmologica*, vol. 119, no. 2, pp. 109–121, Oct. 2009.

[25] C. Kaur, A. Bisht, P. Singh, and G. Joshi, "EEG signal denoising using hybrid approach of variational mode decomposition and wavelets for depression," *Biomed. Signal Process. Control*, vol. 65, Mar. 2021, Art. no. 102337.

[26] L. Chang, R. Wang, and Y. Zhang, "Decoding SSVEP patterns from EEG via multivariate variational mode decomposition-informed canonical correlation analysis," *Biomed. Signal Process. Control*, vol. 71, Jan. 2022, Art. no. 103209.

[27] J. Gilles, "Empirical wavelet transform," *IEEE Trans. Signal Process.*, vol. 61, no. 16, pp. 3999–4010, Aug. 2013.

[28] W. Yan, C. Du, Y. Wu, X. Zheng, and G. Xu, "SSVEP-EEG denoising via image filtering methods," *IEEE Trans. Neural Syst. Rehabil. Eng.*, vol. 29, pp. 1634–1643, 2021.

[29] S. M. M. Safi, M. Pooyan, and A. Motie Nasrabadi, "Improving the performance of the SSVEP-based BCI system using optimized singular spectrum analysis (OSSA)," *Biomed. Signal Process. Control*, vol. 46, pp. 46–58, Sep. 2018.

[30] J. V. Odom et al., "ISCEV standard for clinical visual evoked potentials: (2016 update)," *Documenta Ophthalmologica*, vol. 133, no. 1, pp. 1–9, Aug. 2016.